International Junior Researcher and Engineer Workshop on Hydraulic Structures, 2006, J. Matos and H. Chanson (Eds), Report CH61/06, Div. of Civil Eng., The University of Queensland, Brisbane, Australia - ISBN 1864998687

ADVANCED POST-PROCESSING AND CORRELATION ANALYSES IN HIGH-VELOCITY AIR-WATER FLOWS. 2- MICROSCOPIC PROPERTIES

Hubert Chanson and Giovanna Carosi

Division of Civil Engineering, The University of Queensland, Brisbane QLD 4072, Australia,

h.chanson@uq.edu.au

Keywords: Signal processing, Phase-detection probes, Bubble/droplet clustering, High-velocity air-water flows, Hydraulic structures.

Abstract : The on-going interest in air-water flows is accompanied sometimes by citations of outdated articles and some ignorance of key contributions. A basic issue is the inadequate, incomplete interpretation of air-water flow instrumentation by hydraulic engineers and researchers. This article focus on the bubbly flow structure of high-velocity air-water flow based upon measurements by means of intrusive phase detection probes. It is shown that some advanced post-processing techniques may yield expanded information on the air-water structures and particle clustering.

INTRODUCTION

Air-water flows have been studied relatively recently compared to classical fluid mechanics (Chanson 1997, 2004). The interest in air-water flows is evidenced by a number of associated publications, but it is accompanied sometimes by citations of outdated articles while some fundamental works are ignored. One example is the lack of interest on the microscopic air-water properties of high-velocity flows by hydraulic engineers and researchers.

In this second part, the writers focus on some simple data processing of air-water flow measurements. It is shown that some novel methods yield further information on the air-water microscopic flow properties and air-water bubbly structures. This is illustrated with recent experimental data.

METROLOGY

In high-velocity air-water flows, classical measurement devices like point gauge, Pitot tube, ADV, LDV, are impaired by the entrained air bubbles. For void fractions larger than 2 to 5%, it is acknowledged that the most reliable instrumentation is the phase detection intrusive probe. The needle-shaped probe sensor is designed to pierce the bubbles and droplets as shown in Figure 1A. Figure 1B shows some typical signal outputs of a single-tip probe in skimming flow on a stepped chute. Each steep drop of the signal corresponds to an air bubble pierced by the probe tip. Note that the probe response is not square because of the finite size of the tip, the wetting/drying time of the interface covering the tip and the response time of the probe and electronics.

Phase-detection probes are very sensitive devices, and the sensor must be excited by a high-frequency response electronic system. However, the metrology is susceptible to a number of problems and a systematic quality control is essential. Toombes (2002, pp. 70-72) described in details a number of issues that include some long-term signal decay, probe tip contamination, short-term signal fluctuations caused by debris and water impurities, and electrical noise. A through quality control procedures is essential to ensure meaningful results.

Figure 1 - Phase detection conductivity probe (single-tip design)

(A) Definition sketch

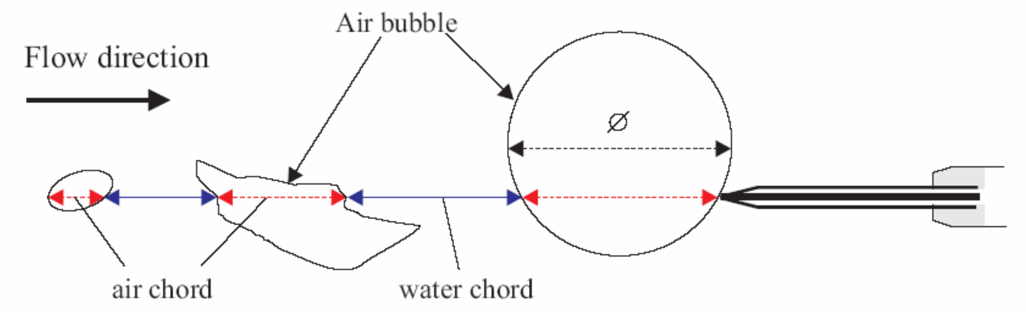

(B) Signal output of a conductivity probe (∅ = 0.25 mm) in skimming flow - d_c/h = 1.33, *Re* = 5.7 E+5, *h* = 0.1 m, θ = 22º, Step edge 10, *y* = 0.022 m, *C* = 0.19, *F* = 167 Hz

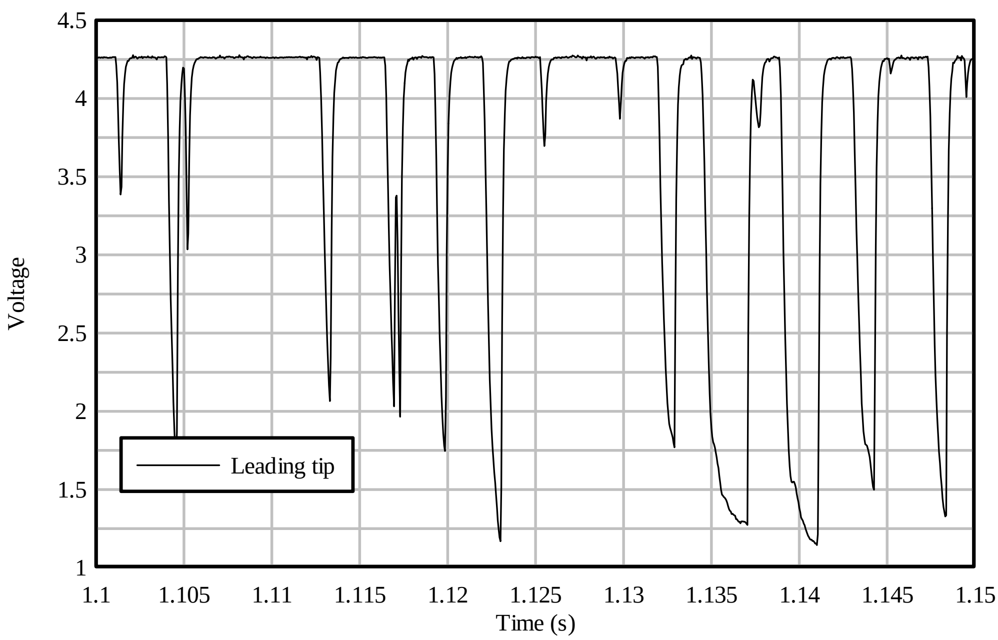

AIR/WATER CHORD DISTRIBUTIONS

In high-velocity air-water flows, most experimental studies present the distributions of time-averaged void fraction and time-averaged velocity (Chanson and Carosi 2006). The void fraction and velocity are some gross parameters that do not describe the air-water structures, the bubbly flow micro-turbulence nor the interactions between entrained bubbles and turbulent shear. Further signal processing may provide additional characteristics on the longitudinal flow structure and bubble clustering.

With a single-tip conductivity probe (Fig. 1), a basic signal processing yields the air/water chord times and their distribution. The air/water chord times are defined as the time spent by the air/water phase on the probe sensor. Bubble chord times are calculated from the thresholded signal (Chanson and Carosi 2006). Statistical analyses of chord time distributions yield the median chord time, standard deviation, skewness and kurtosis of both air and water chord times. Inter-particle arrival times may be also calculated and analysed (see below).

Using the single-tip conductivity probe, the chord time results may be presented in terms of pseudo-bubble/droplet chord sizes *ch* defined as :

$$ch = U_w \times t_{ch} \quad (1)$$

where t_{ch} is the air/water chord time, U_w is the mean flow velocity defined as : $U_w = q_w/d$, q_w is the flow rate per unit width and d is the equivalent clear-water depth defined as :

$$d = \int_0^{Y_{90}} (1 - C) \times dy \quad (2)$$

with y the distance normal to the flow direction and Y_{90} the characteristic distance where the void fraction C equals 0.90. The pseudo chord size (Eq. (1)) is not equal to the air/water chord length because the local interfacial velocity V may differ from the mean flow velocity U_w. But some detailed comparisons in plunging jet flows and skimming flows on a stepped chute showed that Equation (1) overestimated the air/water chord sizes by 2 to 10% in average for $0 \le C \le 0.97$ (Chanson et al. 2006, Carosi and Chanson 2006).

With a double-tip probe, the signal processing yields the air/water chord lengths. The chord size measurement is not a bubble/droplet diameter, but a characteristic streamwise air/water size as sketched in Figure 1A. Figure 2 presents typical results of air/water chord size probability distribution functions in a skimming flow on a stepped chute. The probability distribution functions of chord sizes are analysed in terms of bubble chords in the bubbly flow ($C < 0.3$) and in terms of droplet chords in the spray region ($C > 0.7$). Figure 2 show some normalised chord size distributions. For each graph, the histogram columns represent each the probability of chord size in a 0.5 mm chord interval. For example, the probability of bubble chord from 1 to 1.5 mm is represented by the column labelled 1 mm. Chord sizes larger than 15 mm are regrouped in the last column (> 15). Note that the caption and legend provide the local air-water flow properties (C, F) and probe details.

Figure 2 - Probability distribution functions of chord sizes in skimming flows : d_C/h = 1.45, Step 10, double-tip probe (∅ = 0.25 mm, Δx = 7.0 mm)

(A) Bubble chord size data (C < 0.3)

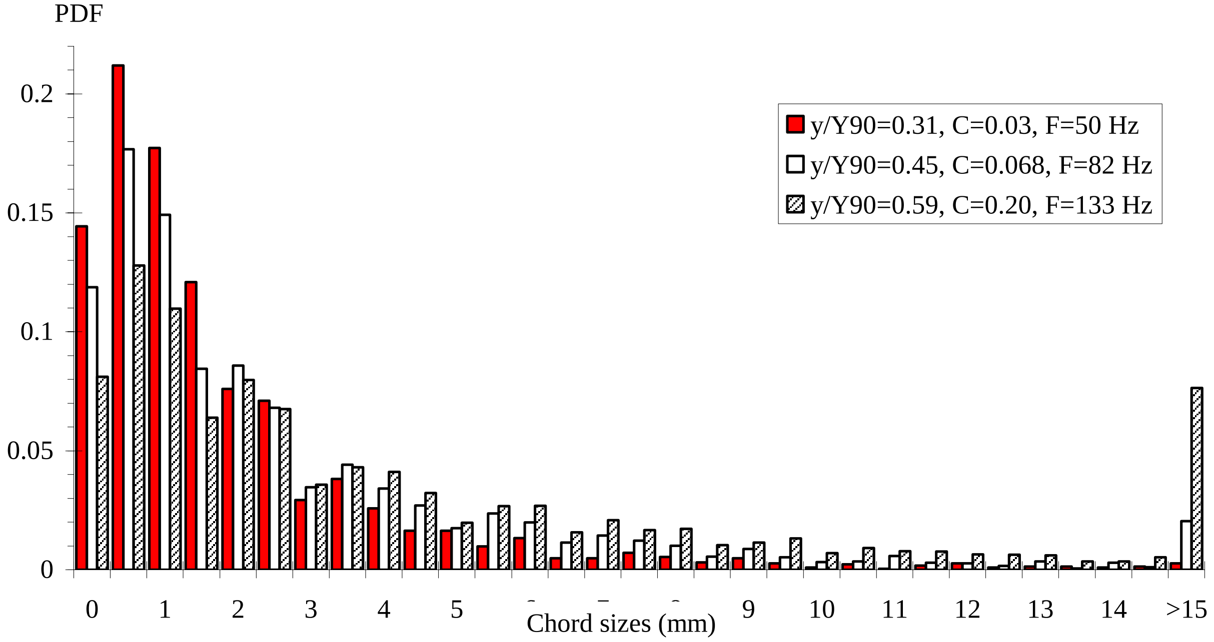

(B) Droplet chord size data (C > 0.7).

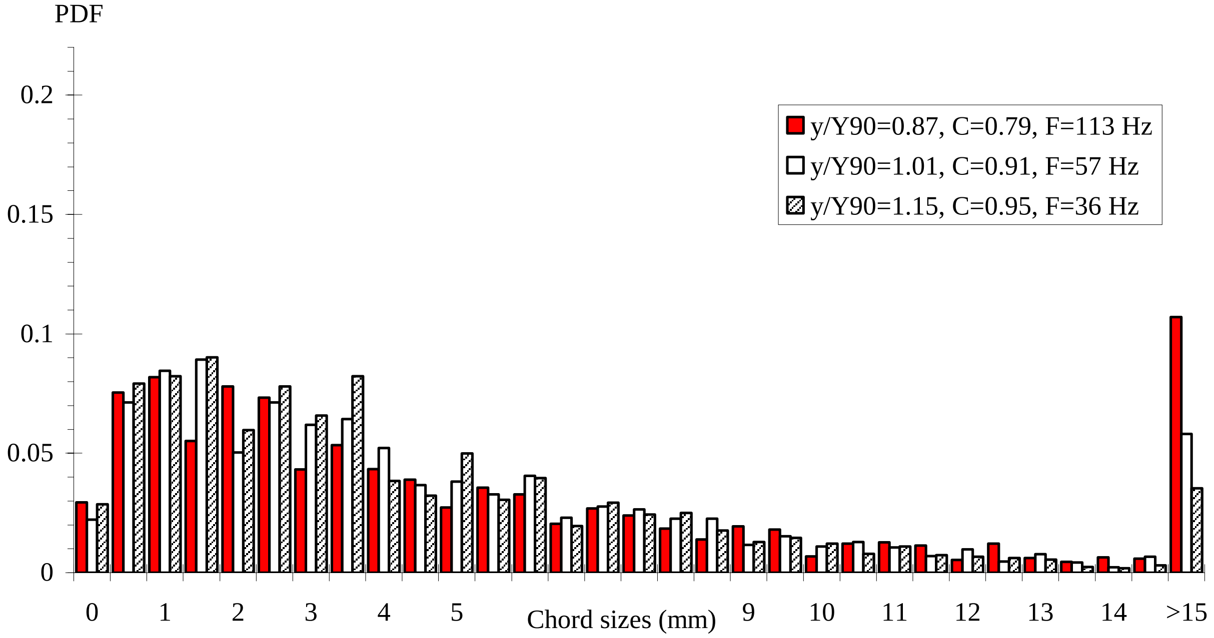

STRUCTURE OF BUBBLY FLOWS

Streamwise particle grouping

With modern phase-detection intrusive probes, some simple signal processing yields the basic statistical moments of air and water chords as well as the probability distribution functions of chord times/sizes. Most experimental results demonstrated a broad spectrum of bubble chords in turbulent shear flows. The range of bubble chord lengths extended over several orders of magnitude including at low void fractions. The distributions of bubble chords were skewed with a preponderance of small bubbles relative to the mean (Fig. 2A). The probability distribution functions of bubble chords tended to follow a log–normal and gamma distributions. Similar findings were observed in a variety of flows encompassing hydraulic jumps, plunging jets, dropshaft flows and high-velocity open channel flows.

In addition, a thorough signal processing may provide some information on the streamwise structure of the air-water flow including bubble clustering. A concentration of bubbles within some relatively short intervals of time may indicate some clustering while it may be instead the consequence of a random occurrence. The study of particle clustering events is relevant to infer whether the formation frequency responds to some particular frequencies of the flow. Figure 3 illustrates some occurrence of bubble pairing in the shear layer of a hydraulic jump. The binary pairing indicator is unity if the water chord time between adjacent bubbles is small (e.g. less than 10% of the median water chord time herein). The pattern of vertical lines seen in Figure 3 is an indication of patterns in which bubbles tend to form bubble groups.

One method is based upon the analysis of the water chord between two adjacent air bubbles. If two bubbles are closer than a particular length scale, they can be considered a group/cluster of bubbles. The characteristic water length scale may be related to the water chord statistics: e.g., a bubble cluster may be defined when the water chord was less than a given percentage of the mean water chord. Another criterion may be related to the leading particle size itself, since particles within that distance are in the near-wake of and may be influenced by the leading particle.

Typical results may include the percentage of bubbles in clusters, the number of clusters per second, and the average number of bubbles per cluster. Extensive experiments in open channels, hydraulic jumps and plunging jets suggested that the outcomes were relatively little affected by the cluster criterion selection (Chanson and Toombes 2002, Chanson et al. 2006, Gualtieri and Chanson 2004). Most results indicated that the longitudinal structure of turbulent flows was characterised by about 10 to 30% of bubbles travelling as parts of a group/cluster, with a very large majority of clusters comprising of two bubbles only. The experimental experience suggested further that a proper cluster analysis requires a high-frequency scan rate for a relatively long scan duration. However the analysis is restricted to the longitudinal distribution of bubbles and does not take into account particles travelling side by side.

A typical result is presented in Figure 4 based upon measurements in the advective diffusion region of a hydraulic jump. Figure 4 shows the vertical distribution of the percentage of bubbles in clusters (lower horizontal axis) and average number of bubbles per cluster (upper horizontal axis) in the hydraulic jump shear layer. The void fraction distribution is also shown for completeness. The criterion for cluster existence was a water chord less than 10% of the median water chord. For this example, about 5 to 15% of all bubbles were part of a cluster structure and the average number of bubbles per cluster was about 2.1.

Figure 3 - Closely spaced bubble pairs in the developing shear layer of a hydraulic jump - Fr_1 = 8.5, $\rho_w \times V_1 \times d_1/\mu_w$ = 9.8 E+4, $x-x_1$ = 0.4 m, d_1 = 0.024 m, y/d_1 = 1.33, C = 0.20, F = 158 Hz (Chanson 2006)

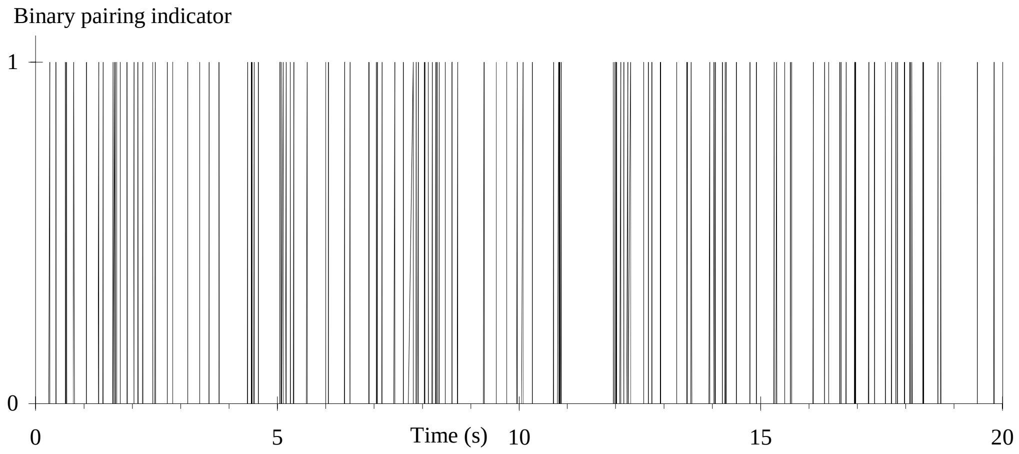

Figure 4 - Bubble clustering in the bubbly flow region of a hydraulic jump: percentage of bubbles in clusters, average number of bubbles per cluster and void fraction - Cluster criterion: water chord time < 10% median water chord time - Fr_1 = 8.5, $\rho_w \times V_1 \times d_1/\mu_w$ = 9.8 E+4, $x-x_1$ = 0.3 m, d_1 = 0.024 m (Chanson 2006)

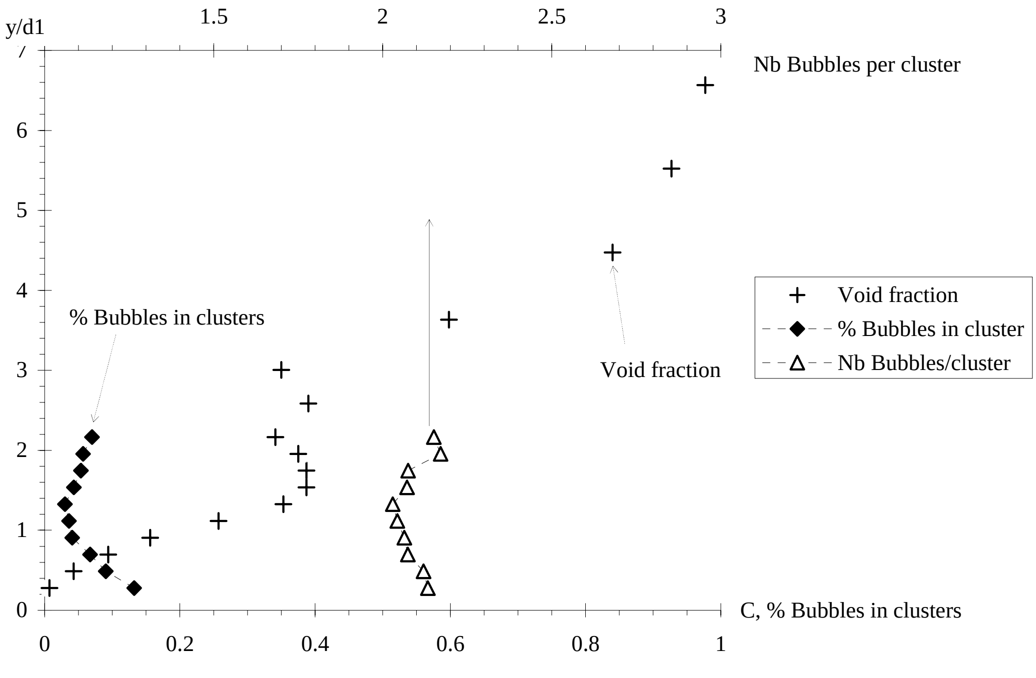

Inter-particle arrival time analysis

For a dispersed phase, a complementary approach is based upon an inter-particle arrival time analysis. The inter-particle arrival time is defined as the time between the arrivals of two consecutive bubbles recorded by a probe sensor fixed in space (Fig. 1B). In other words, it is the time between two successive water-to-air interfaces. The distribution of inter-particle arrival times provides some information on the randomness of the structure. Random dispersed flows are those whose inter-particle arrival time distributions follow inhomogeneous Poisson statistics assuming non-interacting point particles (Edwards and Marx 1995a, Heinlein and Fritsching 2006). In other words, an ideal dispersed flow is driven by a superposition of Poisson processes of bubble sizes, and any deviation from a Poisson process indicates some unsteadiness and particle clustering. That is, the inter-particle time distribution function in steady-random dispersed flows is :

$$f(t) = \frac{\lambda \times (T_{scan} - t) \times \exp(-\lambda \times t)}{\lambda \times T_{scan} - 1 + \exp(-\lambda \times T_{scan})} \qquad (3)$$

where t is the interparticle arrival time, T_{scan} is the sampling duration (herein 45 s), $\lambda = N_{ab}/T_{scan}$ and N_{ab} is the number of particles (Heinlein and Fritsching 2006).

Equation (8) describes an ideal dispersed flow driven by a superposition of Poisson processes of bubble sizes assuming non-interacting particles. Any deviation from a Poisson process indicates some unsteadiness and particle clustering, and the degree of non-random particle clustering may be quantified by Chi-square tests. In practice, the analysis is conducted by breaking down the air-water flow data into narrow classes of particles of comparable sizes that are expected to have the same behaviour (Edwards and Marx 1995b). A simple means consists in dividing the bubble/droplet population in terms of the air/water chord time. The inter-particle arrival time analysis may provide some information on preferential clustering for particular classes of particle sizes.

Some results in terms of inter-particle arrival time distributions are shown in Figure 5 for the same flow conditions and at the same cross-section as the data presented in Figure 4. Figure 5 presents some inter-particle arrival time results for two chord time classes (0 to 0.5 msec. and 3 to 5 msec.). For each class of bubble sizes, a comparison between data and Poisson distribution gives some information on its randomness. For example, Figure 5A shows that the data for bubble chord times below 0.5 msec. did not experience a random behaviour because the experimental and theoretical distributions differed substantially in shape. The second smallest inter-particle time class (0.5-1 msec.) had a population that was 2.5 times the expected value or about 11 standard deviations too large. Such a finding was not seen for medium-sized bubbles with chord times between 3 and 5 msec. (Fig. 5B). This indicates that there was a higher probability of having bubbles with shorter inter-particle arrival times, hence some bubble clustering occurred. Simply the smallest class of bubble chord times did not exhibit the characteristics of a random process.

Figure 5 - Inter-particle arrival time distributions in the bubbly flow region of a hydraulic jump for different classes of air chord times - Comparison between data, Poisson distribution (Eq. (3), solid line) and expected deviations from the Poisson distribution (dashed lines) - Fr_1 = 8.5, $\rho_w \times V_1 \times d_1 / \mu_w$ = 9.8 E+4, $x-x_1$ = 0.3 m, d_1 = 0.024 m

(A) Inter-particle arrival time distributions for bubble chord times between 0 and 0.5 msec., 3055 bubbles, χ^2 = 461

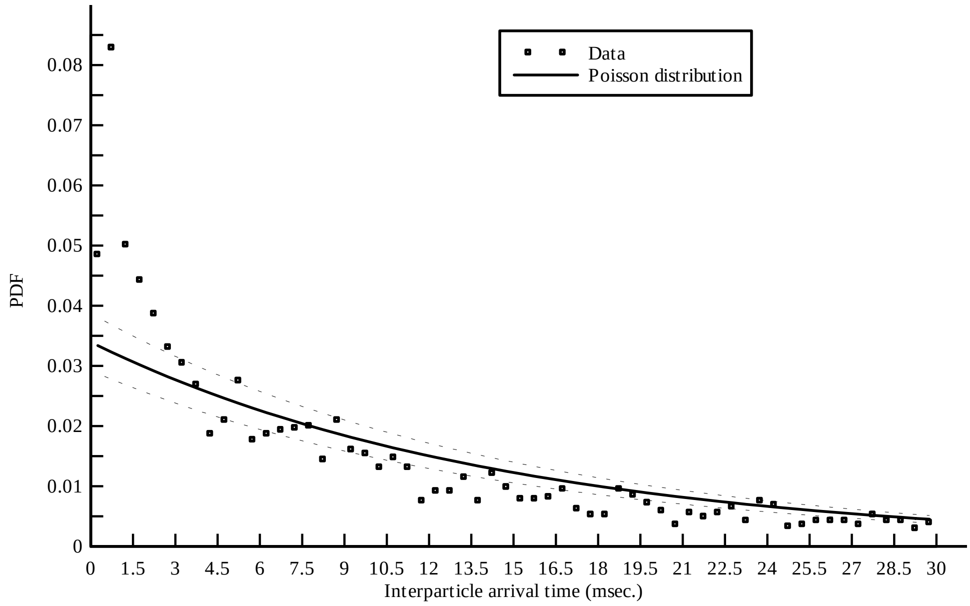

(B) Inter-particle arrival time distributions for bubble chord times between 3 and 5 msec., 581 bubbles, χ^2 = 110

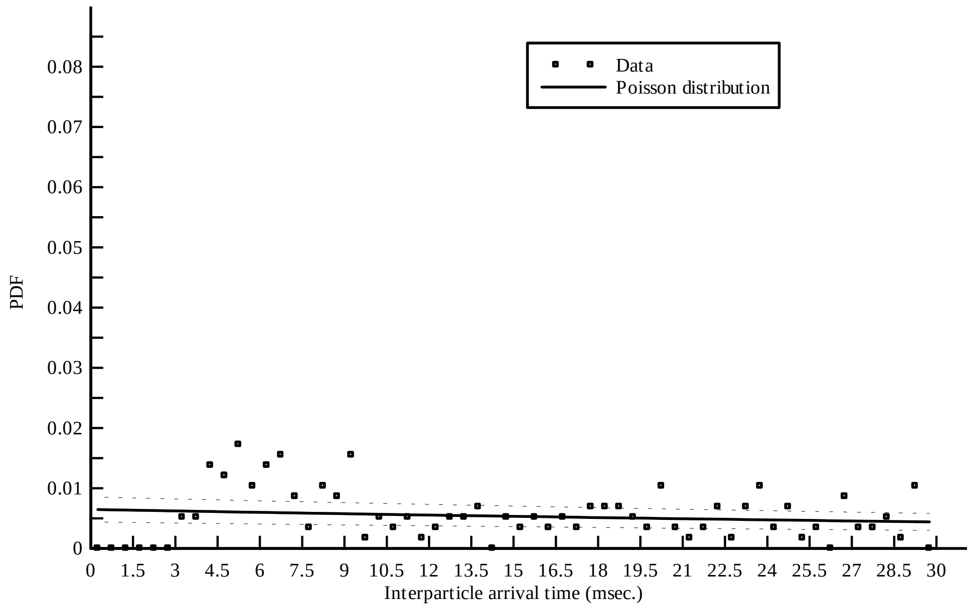

CONCLUSION

In hydraulic engineering, high-velocity air-water flows are characterised by large amounts of entrained air with void fractions commonly larger than 5 to 10%, and air-water velocities greater than 2 to 3 m/s, often between 5 and 40 m/s in prototype spillways. The basic metrology is the intrusive phase detection probe that was used in both laboratory and full-scale studies (Cain and Wood 1981, Chanson 2002). The probe sensor is designed to pierce bubbles and droplets. Some advanced signal processing is developed and the results yield new information on the air-water turbulent structures and particle clustering.

In high-velocity flows, bubble chord distributions showed a broad range of chord times. The distributions were typically skewed with a preponderance of air/water chords smaller than the mean. An analysis of the longitudinal flow structure showed some bubble clustering in the air-water turbulent shear flows. A complementary approach, based upon the inter-particle arrival time analysis, suggested some preferential bubble clustering for small bubble chord times within the investigated flow conditions. Altogether both approaches are complementary, but the inter-particle arrival time analyses give a greater insight into the range of particle classes affected by non-random clustering. This is believed to be a first step towards a better characterisation of air-water flow structures in turbulent shear flows, and the interactions between entrained air and turbulence.

REFERENCES

Cain, P., and Wood, I.R. (1981). "Instrumentation for Aerated Flow on Spillways." *Jl of Hyd. Div.*, ASCE, Vol. 107, HY11, Nov., pp. 1407-1424.

Carosi, G., and Chanson, H. (2006). "Air-Water Time and Length Scales in Skimming Flows on a Stepped Spillway. Application to the Spray Characterisation." *Report No. CH59/06*, Div. of Civil Engineering, The University of Queensland, Brisbane, Australia, July, 142 pages.

Chanson, H. (1997). "Air Bubble Entrainment in Free-Surface Turbulent Shear Flows." *Academic Press*, London, UK, 401 pages.

Chanson, H. (2002). "Air-Water Flow Measurements with Intrusive Phase-Detection Probes. Can we Improve their Interpretation ?." *Jl of Hyd. Engrg.*, ASCE, Vol. 128, No. 3, pp. 252-255

Chanson, H. (2004). "Air-Water Flows in Water Engineering and Hydraulic Structures. Basic Processes and Metrology." *Proc. Intl Conf. on Hydraulics of Dams and River Structures*, Tehran, Iran, Invited Keynote lecture, Balkema Publ., The Netherlands, F. Yazdandoost and J. Attari Ed., pp. 3-16.

Chanson, H. (2006). "Air Bubble Entrainment in Hydraulic Jumps. Similitude and Scale Effects." *Report No. CH57/05*, Dept. of Civil Engineering, The University of Queensland, Brisbane, Australia, Jan., 119 pages.

Chanson, H., Aoki, S., and Hoque, A. (2006). "Bubble Entrainment and Dispersion in Plunging Jet Flows: Freshwater versus Seawater." *Jl of Coastal Research*, Vol. 22, No. 3, May, pp. 664-677.

Chanson, H., and Carosi, G. (2006). "Advanced Post-Processing and Correlation Analyses in High-Velocity Air-Water Flows. 1- Microscopic Properties." *Proc. Intl Junior Researcher and Engineer Workshop on Hydraulic Structures*, IAHR, Montemor-o-Novo, Portugal, 2-4 Sept. 2006.

Chanson, H., and Toombes, L. (2002). "Air-Water Flows down Stepped Chutes : Turbulence and Flow Structure Observations." *Intl Jl of Multiphase Flow*, Vol. 28, No. 11, pp. 1737-1761.

Edwards, C.F., and Marx, K.D. (1995a). "Multipoint Statistical Structure of the Ideal Spray, Part I: Fundamental Concepts and the Realization Density." *Atomization & Sprays*, Vol. 5, pp. 435-455.

Edwards, C.F., and Marx, K.D. (1995b). "Multipoint Statistical Structure of the Ideal Spray, Part II: Evaluating Steadiness using the Inter-particle Time Distribution." *Atomization & Sprays*, Vol. 5, pp. 435-455.

Gualtieri, C., and Chanson, H. (2004). "Clustering Process and Interfacial Area Analysis in a Large-Size Dropshaft." *Proc. 5th Intl Conf. Advances in Fluid Mechanics AFM 2004*, Lisbon, Portugal, March 22-24, Advances in Fluid Mechanics Vol. V, A.Mendes, M.Rahman & C.A. Brebbia Editors, WIT Press, Southampton, UK, pp. 415-424.

Heinlein, J., and Fritsching, U. (2006). "Droplet Clustering in Sprays." *Experiments in Fluids*, Vol. 40, No. 3, pp. 464-472.

Toombes, L. (2002). "Experimental Study of Air-Water Flow Properties on Low-Gradient Stepped Cascades." *Ph.D. thesis*, Dept of Civil Engineering, The University of Queensland, Brisbane, Australia.